JOURNAL OF Materials CHEMISTRY

Organogelators for making porous sol–gel derived silica at two different length scales

G. M. Clavier,[a] J. L. Pozzo,[a] H. Bouas-Laurent,[a] C. Liere,[b] C. Roux[b] and C. Sanchez*[b]

[a]*Photochimie Organique, UMR 5802, U. Bordeaux I, F-33405 Talence, France*
[b]*Laboratoire de Chimie de la Matière Condensée, UMR CNRS 7475, Université Pierre et Marie Curie, F-75252 Paris Cedex 05, France. E-mail: clems@ccr.jussieu.fr*

Received 17th January 2000, Accepted 28th April 2000
Published on the Web 21st June 2000

New sol–gel derived silicas made with a double porous network with pore sizes on two very different length scales (typically several nm and several μm) are reproducibly synthesised using molecular 2,3-di-*n*-decyloxyanthracene (DDOA) organogelators. The micron sized fibrous patterns made in methanol by DDOA aggregates are used as a blueprint for the growing of porous silica fibres. At the same time the mesoporous silica network seems to be templated by smaller DDOA aggregates. By varying the DDOA concentration, the mean size of the mesoporous network increases from 50 to 120 Å and the pore shape changes from a ink-bottle to a cylindrical type.

Introduction

Since the discovery of periodic mesoporous materials,[1] a new era has started in solid state chemistry. This discovery has stimulated research in areas that include studies of sorption and separation, catalysis, formation of intrachannel metal, metal oxide, and semiconductor clusters and inclusion of many metal clusters or other functional guests.[2–4] However, for many applications (*e.g.* catalysis or chromatography) there is also a need to design porous networks (even if the porosity is not periodic) whose porosity can be built on different length scales. Using controlled spinodal phase separation, Nakanishi has recently developed chromatographic stationary phases made of silica having a double porous network on the nanometer and micrometer scales.[5] Assemblies of closely packed latex spheres have also recently been reported to pattern mesoporous metal oxide domains on larger length scales.[6] Simultaneously, Mann has developed a parallel approach that consists of the synthesis of new hierarchical silica based structures made through the use of two templates operating on the nanometer and micrometer scales.[4] The co-assembly of the silica–surfactant mesophase was patterned within a biological superstructure consisting of co-aligned multicellular filaments of *Bacteria subtilis*.

Recently, numerous thermoreversible physical gels formed with low molecular weight organic molecules have been reported.[7] The interest shown for these gels lies in the numerous potential applications envisaged for these materials such as hardeners of solvents, drug delivery systems, membranes, and sensors. More particularly, 2,3-di-*n*-decyloxyanthracene[8] (DDOA) (Fig. 1) exhibits such gelation properties at room temperature in methanol and other solvents when its concentration is in the range of 5×10^{-4} to 10^{-2} mol l^{-1}. The observation of those gels using freeze fracture electron microscopy techniques showed a dense three-dimensional pattern composed of randomly oriented and intertwined micronic fibrous bundles with a 60–70 nm average section for the smallest. Given that the mild characteristics of sol–gel chemistry allow the introduction of fragile organic molecules into an inorganic network,[9–12] we decided to investigate the possible patterning of sol–gel derived silica matrices using DDOA molecules. The present work is focused on the development of systems which contain the same small organic molecule DDOA used as a structure directing agent expressed simultaneously on two different length scales.

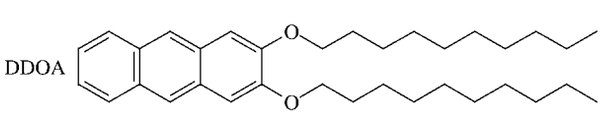

Fig. 1 Molecular structure of 2,3-bis-*n*-decyloxyanthracene.

Experimental

Sample preparation

The silica–DDOA samples were prepared following previously reported procedures for pure silica gels.[9] A solution containing TMOS–MeOH–H_2O (pH = 12.6 or 12.9) in a 1 : 7.73 : 4.05 molar ratio was first prepared: tetramethyl orthosilicate [TMOS, $Si(OCH_3)_4$, Fluka] (4.5 g) and absolute methyl alcohol (CH_3OH, Fluka) (4.5 g) were mixed and added dropwise to a solution containing CH_3OH (4.9 g), ammonium hydroxide (NH_4OH, 28%, Fluka) (0.006 or 0.010 g) and water (2.2 g). This solution (4 mL) was immediately added to a weighed amount of DDOA in a test tube. The tube was septum-capped and then the mixture was sonicated for 10 min, heated at 70 °C until complete dissolution of the organic solid and cooled down to room temperature. The sols containing the DDOA became translucent upon formation of the organic gel, which occurs after *ca.* 20 min. The aggregation process of DDOA molecules responsible for the organic gelation was checked in the DDOA–silica hybrid medium *via* UV-visible experiments. Indeed, after organic gelation the typical 15 nm bathochromic shift[8,13] of the absorption band (located at about 350 nm) corresponding to aggregated organic chromophores was observed. Hydrolysis and condensation reactions of TMOS were catalysed under basic conditions in order to tune the kinetics of formation of the inorganic network with respect to those of the organic gel. When the pH is *ca.* 12.6, the organic translucent gel is formed before the inorganic one (samples labelled A). In contrast, when the pH is *ca.* 12.9, the gelation time t_g of silica can be lowered to about 10 min and consequently the sol gives a *transparent* silica gel before the formation of the *translucent* organic gel, which appears upon cooling down the sample (samples labelled B). The t_g values of the inorganic gels containing the DDOA were the same as those observed for reference samples prepared under the same conditions without DDOA. Five different compositions of

DDOA were prepared and the samples were labelled 0 to 5, the DDOA content increasing with the sample number.

DDOA (0, 2, 4.4, 8 and 15.4 mg) was used for the syntheses of samples 0 to 5 respectively. The final concentrations of DDOA were 0 (A_0 or B_0), 10^{-3} (A_1 or B_1), 2.2×10^{-3} (A_2 or B_2), 4×10^{-3} (A_3 or B_3) and 7.7×10^{-3} M (A_4 or B_4). The samples labelled A_1–A_4 or B_1–B_4 were left to concentrate immediately.

Other gels were also synthesised at pH = 12.6 using the same procedure (the organic gelation occurred before the inorganic one) but were aged for 10 days in a closed vessel before allowing slow evaporation of the solvent. These samples were labelled C.

In an early stage, the samples were washed to remove the organic part and to check the stability of the organic imprint. Soxhlet washing with chloroform was used. The amount of removed DDOA was titrated using UV-vis techniques, which showed organic extraction yields greater than 95%. The three types of sample (A, B and C) were washed and the samples thus obtained were labelled SA, SB and SC respectively.

All the samples were dried in air at room temperature for a few weeks before analysis.

Raman spectroscopy

Raman spectra were recorded with a DILOR Labram 1D Raman Microscope, using a 50X ULWD objective, and 632.8 nm laser excitation allowing a 4 cm^{-1} resolution.

NMR experiments

All nuclear magnetic resonance (NMR) spectra were recorded on a MSL 300 Bruker spectrometer. ^{29}Si magnetic angle spinning (MAS) NMR data were recorded under the following experimental conditions: pulse 2 ms, recycle delay 60 s, spinning frequency 4 kHz. The ^{29}Si NMR spectra were simulated and the signal intensities determined using the WIN-FIT program.[14] The Q^n (n = 0–4) notations have their usual meanings.[15] Q refers to the tetrafunctional central SiO_4 and n indicates the number of the other silicate structures attached to the central unit. The mean degree of condensation c(Q) was calculated using the equation $c(Q)=\Sigma q_j/4$ where q_j is the concentration measured by NMR for Q^j species.

Characterisation of porous structures. Thermogravimetric analysis (TGA) performed on air-dried samples shows a weight loss (2–5%) corresponding to adsorbed solvent between 20 and 140 °C and consequently all samples were heat-treated at 323 K for 12 h prior to analysis.

A scanning electron microscope (STEREOSCAN 120 Cambridge Co.) was employed for the observation of the dried samples. Washed and unwashed samples were used to examine the morphological variations mainly in the micrometer range generated by the elimination of DDOA. Macropores larger than 50 nm can then be observed.

The dried silica gel morphologies were analysed on a smaller length scale using transmission electronic microscopy. The dried material was embedded within a Spurr resin and polymerized at 70 °C over 12 h. After microtomic cutting, ultra thin sections, *ca.* 80–100 nm thick, were observed on a transmission electron microscope (JEOL 100CX II). The distribution of pores smaller than 50 nm was measured by the nitrogen sorption method at liquid nitrogen temperature using an ASAP 2010 (Micromeritics Co.). Samples were degassed at 323 K *in vacuo* for 12 h prior to each measurement. Pore size distributions were determined by the BJH method[16a] for mesopores (pores of radius 2–25 nm). As most of the isotherm loops were of type H2, we used the adsorption branch to evaluate the overall pore size distribution. Nevertheless, such isotherms exhibit features characteristic of very small pores (closure of the loop at $P/P_0=0.42$). Consequently, density functional theory (another approach for evaluating the pore size distribution) was also used to evaluate small pore sizes.[16b] Specific surface areas are obtained by using the BET equation between 0.05 and 0.30 relative pressures.[17] Total pore volumes were determined by the adsorption of nitrogen at a 0.995 relative pressure.

Results and discussions

The samples containing the DDOA have been studied after slow evaporation by optical microscopy coupled with Raman spectroscopy. At this stage, an observation of a typical sample by optical microscopy (Fig. 2a) reveals the presence of numerous interconnected fibres in the dry silica. Raman spectra were recorded in the areas indicated by the circles. The corresponding Raman spectra (Fig. 2b) are clearly distinct and specific for the aggregated DDOA (upper trace, $\nu_a=752$, $\nu_b=1288$, $\nu_c=1396$, $\nu_d=1420$ and $\nu_e=1566$ cm^{-1}) and amorphous silica (lower trace, ν_1(A1) ≈ 814, ν_2(E) ≈ 379, ν_3(F2) ≈ 983 and ν_4 (F2) ≈ 473 cm^{-1}).[18]

A typical ^{29}Si MAS NMR spectrum recorded for a dried sample (A_1) is presented in Fig. 3 and is characteristic of a highly but not fully condensed silica network. The spectrum presents two main resonances at −110 and −101 ppm and a weak resonance at −93 ppm. The first two are assigned to the Q^4 and Q^3 species, respectively, and the last to the Q^2 species. No Q^1 and Q^0 species were detected. The normalised integrated intensities obtained from the simulation of this spectrum are: 69% for Q^4, 30% for Q^3 and 1% for Q^2. The mean degree of condensation c(Q) is equal to 92%. The ^{29}Si MAS NMR spectra recorded for the dried samples exhibit very similar features whatever the synthesis conditions. These NMR experiments show the presence of mainly Q^4 (63–76%) and Q^3 (21–35%) species and a small amount of Q^2 (0–3%). The mean degree of condensation c(Q) is quite the same [(Q) = 92 ± 2%] for all samples because condensation is strongly governed by the basic conditions. The observed small differences in the condensation of silica can probably be

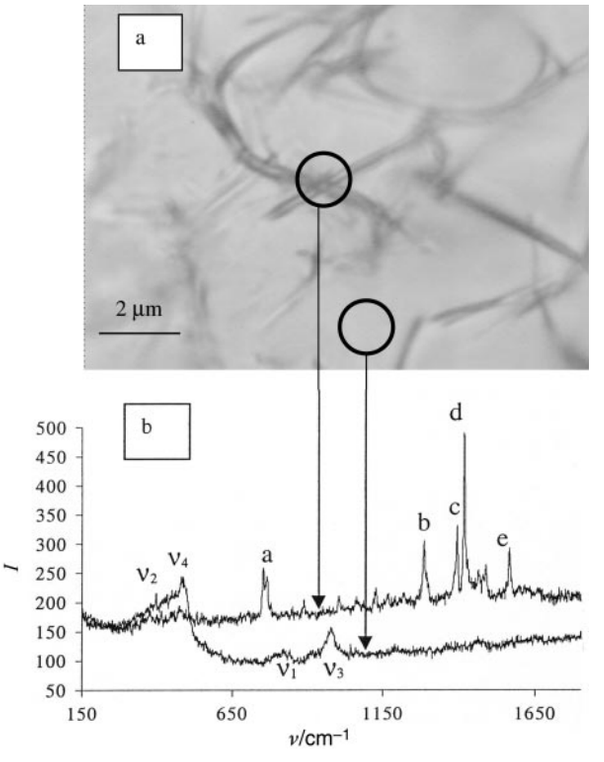

Fig. 2 Optical microscopy coupled with Raman spectroscopy of hybrid gels (sample C).

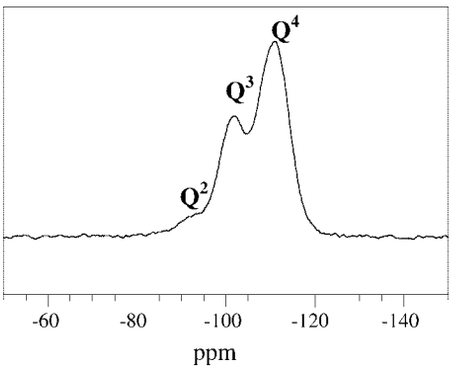

Fig. 3 ^{29}Si MAS NMR spectrum of sample A_1.

related to dissolution–precipitation processes occurring upon ageing before solvent removal.

A typical SEM negative obtained for silica samples containing DDOA is shown in Fig. 4a. Fig. 4b presents the SEM negative of the same sample obtained after Soxhlet washing. SEM experiments clearly show the presence in all the silica–DDOA hybrid samples of the fibrillar micronic structures patterned by the DDOA gelators (Fig. 4a). This is evidence that the anisotropic soft pattern created by the organic gelators is not destroyed by the growth of the stiffer inorganic silica network. Moreover, after extraction of DDOA molecules through Soxhlet washing, the micronic porous fibers imprinted in the silica network are clearly visible (Fig. 4b). In many samples, it has also been observed *via* SEM experiments that the co-alignment of the cylinders of mesoporous silica persists after DDOA extraction.

Moreover, we have recently found that the catalysts used to built the silica network combined with the presence of DDOA improved the patterning of the fibrous texture. A spectacular effect is observed when the gels are synthesised following the well known two step process.[9] In that case TMOS was first hydrolysed in acidic media, then DDOA was added, organic gelation was processed and finally the pH was increased up to

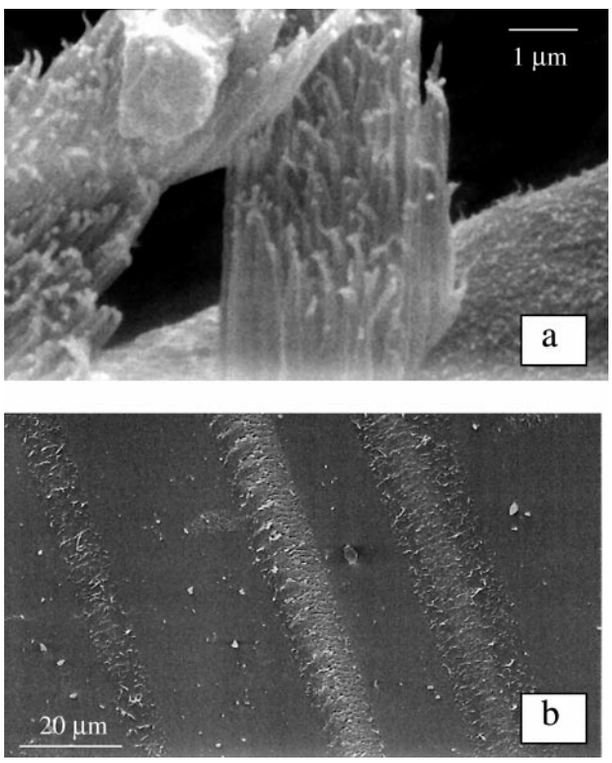

Fig. 4 SEM of silica xerogels: (a) hybrid xerogel with DDOA (samples A, B or C); (b) xerogel after DDOA extraction (samples SA, SB or SC).

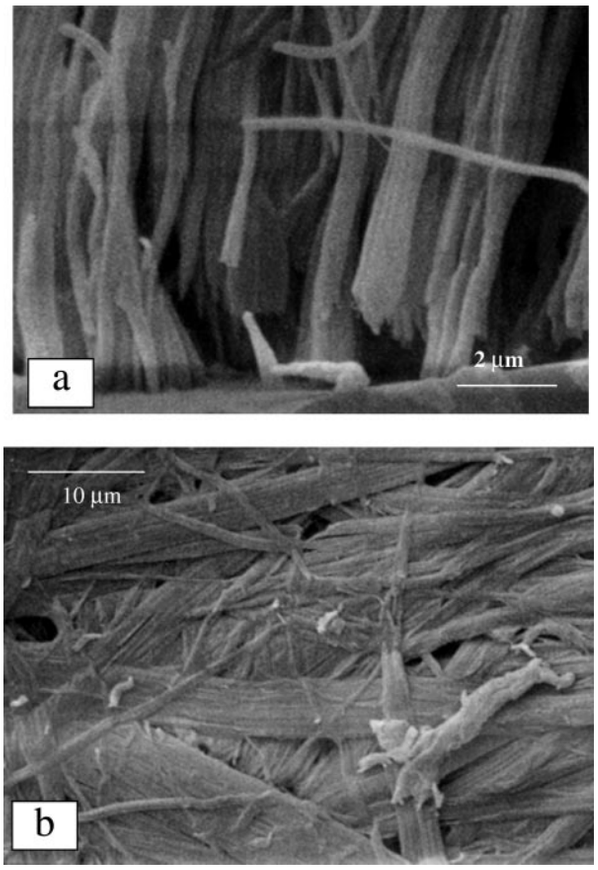

Fig. 5 SEM of silica xerogels: (a) two-step hybrid xerogel with DDOA; (b) one-step xerogel with DPOA.

12.6 with NH_4OH. The final DDOA concentration was 4.2×10^{-3} M. Fig. 5a shows a typical SEM obtained for this new sample. The SEM picture exhibits features typical of well-grown fibrous silica that is forming a three-dimensional network structure. The diameter of the fibres is *ca.* 200 nm. Most of the fibres are co-aligned and practically no amorphous silica network is observed, indicating the large volume fraction occupied by the fibrous network.

These results are reproducible and indicate that the fibrous silica matrix is patterned by the DDOA fibrous aggregates. These results are in agreement with previous publications showing that DDOA forms fibrous bundles,[8] and that the silica matrix can be patterned within aligned bacterial filaments.[4] They suggest the presence of some interaction between the silicate species and the gelator molecules. Since DDOA is not charged, but instead contains a weakly polar head made with an oxygen-terminated anthracenic moiety, it is thought that the oligomeric silica species were gathered around the framework of the organogelator *via* interactions which are probably weakly hydrophobic at high pH. However, in acidic medium these interactions may be governed by hydrogen bonding. The large amount of textured fibres observed in the silica gels made *via* a two step process can probably be related to the fact that silica–gelator interactions are stronger at low pH, and template more efficiently the growing silica network during the first step of the process. The matching of the interactions between the organogelator and the silica network is subtler than the one expected for traditional surfactants that exhibit a strong amphiphilic character. Qualitatively these interactions allow the formation of the fibrous texture of the precipitated silica. On the other hand, the sol–gel conditions allow modification of the organisation of the network.

Some preliminary experiments performed on the growth of silica in the presence of organogelators such as 2,3-di-*n*-alkoxyphenazines,[19] whose amphiphilic character (amino

groups are located inside the anthracenic rings) is more pronounced, show a high density of interwined micronic fibrous bundles of silica (see SEM in Fig. 5b). These new silica–organogel hybrid systems are currently under investigation; they will probably help us shed light on the nature of the interaction between these anthracene based organogelators and the growing silica network. The use of organogels for the patterning of inorganic networks has also been reported very recently by Japanese research groups.[20,21] At the end of 1999 it was reported that titania fibres[20] or even chiral hollow silica fibres[21] with a helical structure can also be synthesised *via* the sol–gel process using as templates organogels made from *N*-benzyloxycarbonyl-L-isoleucylaminooctane or cholesterol derivatives respectively.

TEM observations made on all the samples (A or B) in the form of thin sections (80–100 nm thick) revealed the conventional granular silica structure. These materials are made of amorphous mesoporous silica, as confirmed by X-ray scattering experiments, which do not show any correlation peaks typical of periodic mesoporous networks, and through nitrogen adsorption–desorption experiments (*vide infra*).

The effect of DDOA molecules on pore size and distribution can be evidenced in the study performed on hybrid DDOA–silica gels that were left to concentrate immediately (A and B samples). Isotherm plots and BJH adsorption pore distributions are presented in Fig. 6 for three typical samples: the pure silica network (B_0 or A_0 samples, pH = 12.9 or 12.6), a hybrid DDOA–silica network containing [DDOA] = 10^{-3} mol l^{-1} where the organic gelation occurs before inorganic gelation (A_1 sample), and a hybrid DDOA–silica network containing [DDOA] = 10^{-3} mol l^{-1} where the gelation of the organic part occurs after the inorganic part (B_1 sample). All plots correspond to type IV isotherms in the Brunauer classification. Characteristic features of the type IV isotherm plots are its hysteresis loop, which is associated with the filling and emptying of mesopores by capillary condensation. The loop is of type H2 associated with an interconnected network of pores of different size and shape. For all samples the specific areas are in the range 500–600 $m^2 g^{-1}$. However, the pore size and distribution are strongly dependent on the gelation procedure. The A_0 and B_0 reference samples show an average pore diameter of about 33 Å (Fig. 6a). It should be noted that DFT analysis, which is more valid in this range of pore size, gives the same average pore diameter. The maximum of the pore size diameter is centered around 40 Å and the porous volumes are equal to about 0.4–0.5 $cm^3 g^{-1}$. However, when DDOA leads to organic gelation prior to the formation of an inorganic network the resulting mesoporous silica network is strongly modified. Indeed, the pore size distribution is broader and the average pore diameter and pore volume increase to values of *ca.* 62 Å and 0.75 $cm^3 g^{-1}$ respectively (Fig. 6b). The maximum of the pore size diameter is close to 100 Å. Moreover, when the gelation of the organic component occurred after that of the inorganic part (B_1 sample), the isotherm shows a narrower bimodal mesoporous distribution with an average pore diameter at 42 Å and a pore volume equal to about 0.5 $cm^3 g^{-1}$ (Fig. 6c). These values are lower than those obtained for sample A_1 and close to those obtained for samples A_0 and B_0. The pore size distribution shows a maximum centered around 40 Å and a shoulder located around 90 Å. The pore size maximum corresponds to the one found for samples A_0 and B_0 whereas the pore size for the shoulder is close to that for the sample A_1. These experiments clearly illustrate the effect of the DDOA molecules on the mesoporous structure.

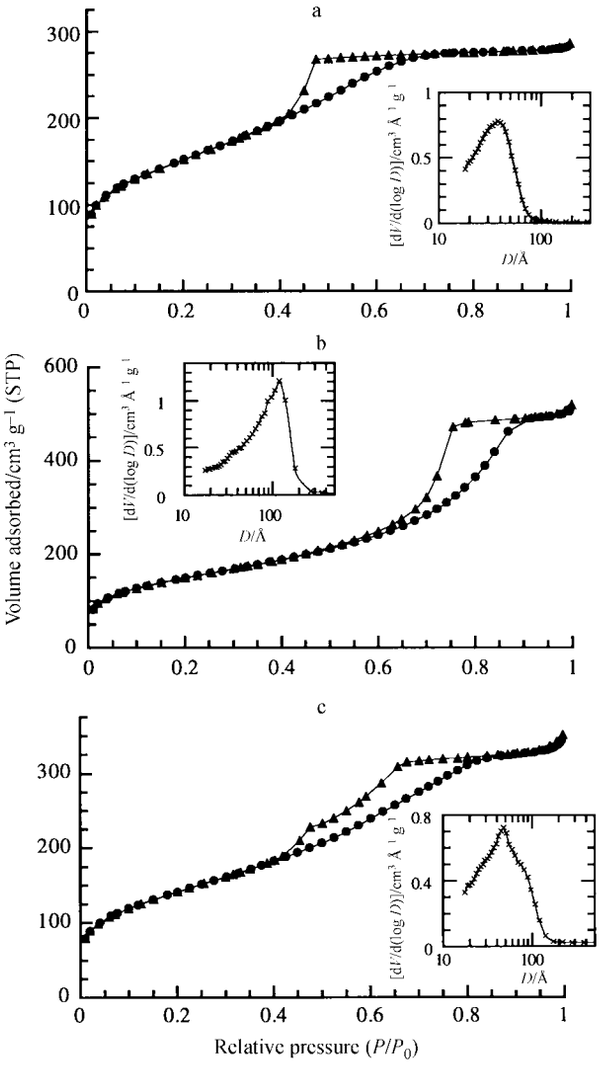

Fig. 6 Typical N_2 isotherms (● adsorption, ▲ desorption) and BJH distributions of three silica xerogels: (a) [DDOA] = 0 M, pure inorganic gel (samples A_0 or B_0); (b) [DDOA] = 10^{-3} M, organic gelation occurs before the inorganic one (sample A_1); (c) [DDOA] = 10^{-3} M, organic gelation occurs after the inorganic one (sample B_1).

Isotherm plots and BJH adsorption pore distributions are presented in Fig. 7a–b for samples SA_1 and SB_1, which correspond to the samples obtained after Soxhlet washing of samples A_1 and B_1. Both plots also correspond to type IV isotherms typical of mesoporous materials, but the BJH adsorption distributions are different. The distribution obtained for sample SA_1 (Fig. 7a) is sharp, whereas the one obtained for sample SB_1 (Fig. 7b) is much broader. For sample SA_1 the average pore diameter D, the pore volume Vp and the specific surface area S are $D_{SA1} = 68$ Å, $Vp_{SA1} = 0.8$ $cm^3 g^{-1}$ and $S_{SA1} = 509$ $m^2 g^{-1}$, respectively. These values are close to those obtained for the non-washed sample A_1 ($D_{A1} = 62$ Å, $Vp_{A1} = 0.75$ $cm^3 g^{-1}$ and $S_{A1} = 510$ $m^2 g^{-1}$). This observation indicates that the Soxhlet washing does not have a significant influence on the mesoporous network when the formation of the inorganic network is performed after the organic gelation. However, when the gelation of the organic part occurred after the inorganic one (SB_1 samples), the washing procedure yields an opposite effect, altering the mesoporous network (Fig. 6c for sample B_1 and Fig. 7b for sample SB_1). After washing, the average pore diameter increases slightly (from 42 to 56 Å) while the pore volume and the specific area increase significantly (from 0.5 to 0.95 $cm^3 g^{-1}$ and from 490 to 730 $m^2 g^{-1}$, respectively). These values tend towards those obtained for the washed samples SA_0 and SB_0 made without DDOA ($D_{SB0} = 74$ Å, $Vp_{SB0} = 1.3$ $cm^3 g^{-1}$ and $S_{SB0} = 740$ $m^2 g^{-1}$). Consequently, the formation of the organic gel after the inorganic silica gel does not avoid the structural evolutions of the mesoporous silica network generated upon Soxhlet washing.

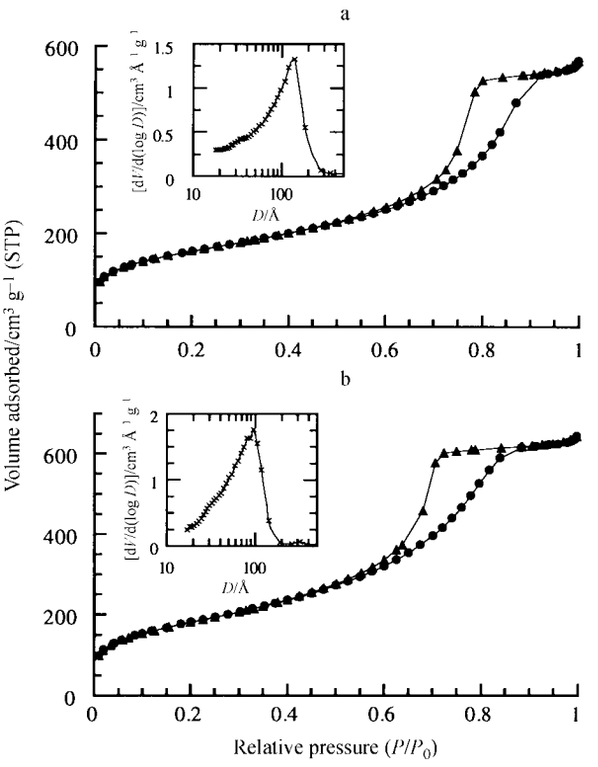

Fig. 7 Typical N_2 isotherms (● adsorption, ▲ desorption) and BJH distributions of two washed silica xerogels: (a) [DDOA] = 10^{-3} M, organic gelation occurs before the inorganic one (sample SA_1); (b) [DDOA] = 10^{-3} M, organic gelation occurs after the inorganic one (sample SB_1).

In the basic medium used for our experiments, redissolution–precipitation of silica species has been found to occur upon ageing. As a consequence isotherm plots and BJH adsorption pore distributions strongly depend on the ageing of the samples. The general observed tendency is for an increase of the specific area to 600–700 m^2 g^{-1} for samples aged 10 days at pH = 12.6. However, there is a net influence of the DDOA concentration on the pore size and pore shape. The pore size evolution can be illustrated with the data presented in Table 1, which correspond to four silica gels for which organic gelation has taken place before inorganic gelation; the gels were aged 10 days and DDOA molecules were eliminated through Sohxlet washing (samples SC). For these samples, the mean surface area does not vary with the DDOA concentration within experimental error. However, the mean pore size and pore volume increase with increasing DDOA concentration. The mean pore size increases from 50 to 120 Å. Moreover, we observed an evolution of the hysteresis loop with the DDOA loading. At low DDOA concentration the hysteresis loop is close to the ones obtained at short ageing time (Figs. 6 and 7). It is of type H2, indicating the presence of ink-bottle shaped pores. However, at high DDOA concentration the hysteresis loop is close to type H1, characteristic of pores having a more cylindrical shape.

The mechanism controlling the evolution of the mesoporosity with the DDOA concentration is not yet clearly understood. Small aggregates of DDOA a few nanometers in size, the size of which vary with the DDOA concentration, may be present in equilibrium with the longer fibrous aggregates forming the organogels. These small aggregates trapped in the silica generate a mesoporous network which mean the size and shape thus depend on DDOA concentration.

Conclusions

This work illustrates how the same molecule can allow the fabrication of different new sol–gel derived silicas. We have shown that SiO_2 fibres are created by the interaction of the fibrous aggregates built from DDOA molecules and the growing silica network. The texturation and co-alignment of the fibres seem to be favoured by a two step process that starts in acidic medium or by the use of anthracenic gelators such as 2,3-di-*n*-alkoxyphenazines,[14] for which the amphiphilic character is more pronounced.

Moreover, the DDOA organogelator molecules also have a noticeable influence on the mesoporosity of the resulting silica network: (i) the mesoporous networks of non-aged silica gels obtained after formation of the organogel can be stabilised against evolutions that may occur during Soxhlet washing procedures; and (ii) the pore size of aged silica gels increases from about 50 to 120 Å with increasing DDOA concentration (the pore shape changes from ink-bottle to cylindrical type).

The origin of these effects on the mesoporosity is not yet clearly understood. Future work will thus be devoted to obtaining systems which present a higher degree of organisation. In this sense, organogelators having more pronounced surfactant properties than DDOA may help to build model hybrid systems.

Acknowledgements

We would like to thank Dr F. Placin for assistance with optical microscopy and Raman spectroscopy measurements.

References

1 J. S. Beck, J. C. Vartuli, W. J. Roth, M. E. Leonowicz, C. T. Kresge, K. D. Schmitt, C. T.-W. Chu, D. H. Olson, E. W. Sheppard, S. B. MacCullen, J. B. Higgins and J. L. Schlenker, *J. Am. Chem. Soc.*, 1992, **114**, 10834.
2 K. Moller and T. Bein, *Chem. Mater.*, 1998, **10**, 2950.
3 C. G. Göltner and M. Antonietti, *Adv. Mater*, 1997, **9**(5), 431.
4 S. Mann, S. L. Burkett, S. A. Davis, C. E. Fowler, N. H. Mendelson, S. D. Sims, D. Walsh and N. T. Whilton, *Chem. Mater.*, 1997, **9**, 2300.
5 B. T. Holland, C. F. Blanford, T. Do and A. Stein, *Chem. Mater.*, 1999, **11**, 795.
6 K. Nakanishi, *J. Porous Mater.*, 1997, 67.
7 P. Terech and R. G. Weiss, *Chem. Rev.*, 1997, **97**, 3133.
8 T. Brotin, R. Utermöhlen, F. Fages, H. Bouas-Laurent and J. P. Desvergne, *J. Chem. Soc., Chem. Commun.*, 1991, 416.
9 C. J. Brinker and G. Scherrer, *Sol–Gel Science, the Physics and Chemistry of Sol–Gel Processing*, Academic Press, San Diego, 1989.
10 C. Sanchez and F. Ribot, *New J. Chem.*, 1994, **18**, 1007.
11 C. Sanchez, F. Ribot and B. Lebeau, *J. Mater. Chem*, 1999, **9**, 35.
12 Y. Ono, K. Nakashima, M. Sano, Y. Kanekiyo, K. Inoue, J. Hojo and S. Shinkai, *Chem. Commun.*, 1998, 485.

Table 1 Evolution of the mean pore diameter, pore volume and surface area with DDOA concentration for Soxhlet washed silica xerogels (samples SC) (pH = 12.6, aged 10 days)

Sample	[DDOA]/mol L^{-1}	Mean pore diameter/Å	Porous volume/cm^3 g^{-1}	Surface area/m^2 g^{-1}
SC_0	0	74	1.29	740
SC_1	1.0×10^{-3}	48	0.82	690
SC_2	2.2×10^{-3}	62	0.88	615
SC_3	4.0×10^{-3}	100	1.50	655
SC_4	7.7×10^{-3}	114	1.68	640

13 J.-P. Desvergne, F. Fages, H. Bouas-Laurent and P. Marsau, *Pure Appl. Chem.*, 1992, **64**, 1231.
14 D. Massiot, H. Thiele and A. Germanus, *Bruker Rep.*, 1994, **140**, 43.
15 R. H. Glaser, G. L. Wilkes and C. E. Bronnimann, *J. Non-Cryst. Solids*, 1989, **113**, 73.
16 (*a*) E. P. Barrett, L. G. Joyner and P. H. Halenda, *J. Am. Chem. Soc.*, 1951, **73**, 373; (*b*) J. P. Olivier, *J. Porous Mater.*, 1995, **2**, 9.
17 S. Brunauer, P. H. Emmett and E. Teller, *J. Am. Chem. Soc.*, 1938, **60**, 309.
18 R. A. Condrate, *J. Non-Cryst. Solids*, 1986, **84**, 26.
19 J.-L. Pozzo, G. M. Clavier and J.-P. Desvergne, *J. Mater. Chem*, 1998, **8**, 2575.
20 S. Kobayashi, K. Hanabusa, M. Susuki, M. Kimura and H. Shirai, *Chem. Lett.*, 1999, 1077.
21 Y. Ono, K. Nakashima, M. Sano, Y. Kanekiyo, K. Inoue and J. Hojo, *Chem. Lett.*, 1999, 1477.